Solar Energy Materials & Solar Cells 106 (2012) 17–21

Contents lists available at SciVerse ScienceDirect

Solar Energy Materials & Solar Cells

journal homepage: www.elsevier.com/locate/solmat

Interface properties of a-SiN$_x$:H/Si to improve surface passivation

Machteld W.P.E. Lamers [a,*], Keith T. Butler [b], John H. Harding [b], Arthur Weeber [a]

[a] ECN Solar Energy, PO Box 1, ZG Petten 1755, Netherlands
[b] University of Sheffield, Western Bank, Sheffield S10 2TN, United Kingdom

ARTICLE INFO

Available online 5 July 2012

Keywords:
Silicon nitride
Passivation
V_{oc}
PECVD
Nitridation
Fixed charge

ABSTRACT

Nitridation is the process in which, during the initial growth of a-SiN$_x$:H layers on Si surfaces, nitrogen is incorporated into the Si lattice near its surface. We show that this nitridation process affects the density of interface states (D_{it}) and fixed charges (Q_f) at the interface. These parameters determine the effective surface passivation quality of the layers. The nitridation can be tuned independently of the growth of a-SiN$_x$:H layers by using a plasma treatment prior to actual a-SiN$_x$:H layer deposition. It is shown that Q_f can be varied from 2×10^{12} to 15×10^{12} cm^{-2} without changing the a-SiN$_x$:H deposition process. It is demonstrated that in our case and processing window, Q_f is the determining factor in surface passivation quality in the range of 2×10^{12} to 8×10^{12} cm^{-2}. For higher values of Q_f, D_{it} has increased significantly and has become dominant thereby reducing the passivation quality. It is shown that the passivation can be controlled independently of the a-SiN$_x$:H deposition process. In completed solar cells the effect of the controlled Q_f and D_{it} is studied. On n-type solar cells, due to increased depletion, increases in Q_f and D_{it} resulted in a drop in open-circuit voltage, V_{oc}, of over 20 mV. On p-type solar cells, where the Q_f results in accumulation, the effect was negligible.

1. Introduction

Hydrogenated amorphous silicon nitride (a-SiN$_x$:H) is the standard antireflection and passivating layer, for both surface and bulk defects, in wafer-based silicon solar cells. Commonly, the layer is deposited using plasma-enhanced chemical vapor deposition (PECVD). The physical properties of the layer have previously been correlated to cell output properties like the open-circuit voltage V_{oc} [1,2]. In general, the optimized a-SiN$_x$:H layer is a compromise of optical (antireflection and absorption) properties, and bulk and surface passivation. Si-rich a-SiN$_x$:H layers show good surface passivation, but are highly absorbing and cannot be used for solar cell application. N-rich layers show good optical properties, but are less effective in surface passivation. In this paper our aim is to better understand the surface passivating properties and open ways to de-couple the surface passivating properties from the other properties (bulk passivation and optical) that should finally result in better solar cells. A qualification is made of the effect of surface passivation on solar cells depending on the dopant type and doping density at the surface, and independent of bulk passivation.

The total surface passivation is determined by the combined effect of two mechanisms: so-called chemical passivation by reducing the density of interface states (D_{it}) and field-effect passivation by the number of fixed charges (Q_f) at the interface with Si. A low D_{it} reduces the recombination rate at the interface. For Q_f the effect on surface passivation depends, besides other parameters, on the doping type and doping density [3]. For lightly doped material a high Q_f will increase the field-effect contribution to the surface passivation. For doping types with opposite polarity than the fixed charges, the field effect is governed by accumulation. For doped material with the same polarity the field effect is governed by inversion. For highly doped materials with opposite polarity as the fixed charges, a higher Q_f can (slightly) improve the surface passivation by accumulation. For highly doped materials with the same polarity as Q_f the surface passivating quality will decrease because of depletion. More information can be found in [3].

As Q_f and D_{it} are properties of the interface of a-SiN$_x$:H/Si, this indicates that they are determined by the initial growth of the a-SiN$_x$:H layer. More profoundly, Q_f is related to the interface structure between the materials (a-SiN$_x$:H and Si) causing a local-field effect as was described by Aspnes [4]. This local field depends on the different polarizabilities of each material and the variation in volume density of these polarizabilities over distance at the interface. The different components in bulk a-SiN$_x$:H, which can be charged have been linked to the so-called K- and N-centers [5]. These centers are respectively $*Si{\equiv}N_3$ and $*N{=}Si_2$. $*$ indicates that these centers can be neutral, positive, negative or bonded to H. Assuming that K- and N-centers also

* Corresponding author. Tel.: +31 88 515 56 4718; fax: +31 88 515 8214.
E-mail address: lamers@ecn.nl (M.W.P.E. Lamers).

0927-0248/$ - see front matter © 2012 Elsevier B.V. All rights reserved.
http://dx.doi.org/10.1016/j.solmat.2012.06.025

occur at the interface, this leads to the conclusion that Q_f is determined by the variation and volume fractions of K- and N-centers at the interface region of a-SiN_x:H/Si. The number of K-centers that is bonded to H can be estimated from the Si–H peak in a Fourier transform infrared spectroscopy (FTIR) [6] spectrum and is correlated to Q_f and D_{it}. A peak location close to 2220 cm^{-1} indicates relatively more K-centers. Both the K- and N-centers have also been described as the origins of the dangling bonds at the interface and therefore related to D_{it} [5]. Therefore, when the concentration of (charged) K- and/or N-centers increases, Q_f increases correspondingly. Simultaneously, as the volume fraction of the centers is increased, the amount of (unpassivated) dangling bonds also increases and, therefore, D_{it} increases as well. Additionally, it is shown in this paper that the Q_f might also be connected to local distortions in the SiN_x:H.

a-SiN_x:H, as described in this article, is deposited using remote-PECVD. In the plasma the process gases, typically SiH_4 and NH_3, are dissociated. Subsequently, a thin film a-SiN_x:H can now grow on the substrate surface. During the initial growth of a-SiN_x:H the surface is nitridated, which can be described as N-insertion into the Si surface. The interface region itself is approximately found to be 1–3 nm wide. Depending on the deposition temperature and gas flow of NH_3 different bonds and nitridation characteristics are obtained [7]. Up to temperatures of 300 °C no effect was observed. Above 350 °C it is observed that $-NH_2$ starts to adhere to the Si surface. Above 400 °C N begins to be inserted into the Si–Si bonds. Above 425 °C silicon nitride is formed at the Si surface whose formation increases with temperature. That this nitridation has indeed a direct relation with Q_f was shown by Takakura, though he did not observe a difference in D_{it} [8].

In this article we will demonstrate the variations in Q_f and D_{it} for different SiN_x:H layers. Additionally, we show that different plasma pretreatments prior to SiN_x:H deposition cause different nitridation profiles and thus different surface passivating properties while applying the same a-SiN_x:H layer. The effect of the nitridation on the surface passivating properties for completed solar cells is shown as well. This indicates that separate control of bulk and interface properties of a-SiN_x:H is possible.

2. Layer study

2.1. General SiN_x:H

During a-SiN_x:H deposition, different gas ratios and temperatures determine both the initial growth conditions and bulk properties [1,9,10]. As the initial growth of the a-SiN_x:H layer determines both nitridation and the Q_f and D_{it} values, a clear correlation is found between the properties of the layer and Q_f and D_{it}. To show this, samples were prepared using 275 μm thick p-type FZ ⟨1 0 0⟩ wafers, which were double side mirror polished with a base resistivity of 2.5 Ω cm. Remote PECVD was used to deposit 80–100 nm a-SiN_x:H layers with different composition on one side of the wafer. Deconvoluted bond densities were calculated from FTIR data, and after 300 nm aluminum deposition on the samples to create Metal-Insulator-Silicon (MIS) structures, Q_f and D_{it} were determined using Capacitance-Voltage (CV) MIS analysis. The relationships between the Si–H bond density in the H–Si–N_3 configuration (at 2220 cm^{-1}), the total Si–H bond density, the N–H bond density, the Si–N bond density in the locally distorted configuration (at 790 cm^{-1}), the refractive index n (at 633 nm as determined with ellipsometry), the effective surface recombination velocity (SRV) and Q_f are shown in Fig. 1A and B. Additionally, we find a clear and positive correlation between Q_f and D_{it} as can be seen in Fig. 1B and in [10]. A similar relationship between n, the Si–H bond density in the H–Si–N_3 configuration and the Si–N bond density in the locally distorted configuration was described in [11] and a similar trend between n and Q_f was found in [12]. The results obtained in literature regarding the exact conversion values needed to convert the area of the FTIR spectrum per bond to a density is not conclusive, therefore we decided to show the data in peak area of the bond density [13]. The Q_f found in our experiments is relatively high. To confirm the validity of the results, a comparison was done with SiN_x:H fabricated with a batch PECVD, which showed similar values as obtained in [11]. Also, reference Al_2O_3 layers were measured and comparative values were obtained.

With increasing N content in the layer, corresponding to a decreasing n, Q_f increases. This can be explained since, as the number of charged K-centers increases, the neutral dangling bonds (uncharged and non-passivated K-centers) increase as well. However, as the N-content in the SiN_x:H layer increases further ($n < 2-2.1$) the layer becomes less distorted as the Si–N bond density at 790 cm^{-1} shows a steep decrease; additionally the layer shows a sharp increase in N-H bond densities while the Si–H peak is very small or no longer observed in the FTIR spectrum. For these layers the amount of dangling K-centers decrease as the distortion lowers, as consequently Q_f reduces. The effective SRV is a combined effect of Q_f and passivation of dangling Si bonds by H (high Si–H bond density). For optimal light management of a solar cell, the refractive index should be around 2.05 [14,15]; for optimal bulk passivation a Si–N bond density of 1.2–1.3 × 10^{23}/cm^3, which corresponds to a total area bond density of 560–580/

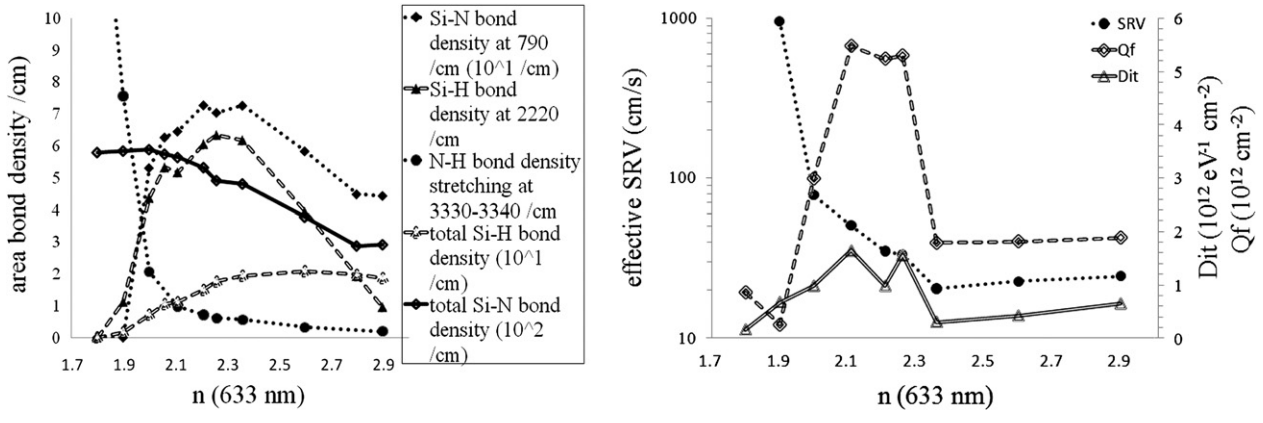

Fig. 1. (A) Relationship between (the peak areas of) the Si–H bond density, the deconvoluted Si–H bond density at 2220 cm^{-1}, the Si–N bond density, the deconvoluted Si–N bond density at 790 cm^{-1} (distorted), N–H bond density and n. (B) Relationship between the effective surface recombination velocity (SRV), Q_f and n.

cm, is necessary in combination with sufficient N–H bonds [1,2,16]; these requirements can be met simultaneously but do not provide a low effective SRV as is clear from Fig. 1A and B. To tune the effective SRV separately from the bulk properties, we focus on changing the N content (and thus K-centers) at the surface by tuning the nitridation prior to the bulk SiN_x:H layer deposition.

2.2. Nitridation of the Si surface

To study the effect of nitridation on passivation in more detail, various NH_3 plasma (pre-) treatments prior to a-SiN_x:H layer deposition were done. To study possible dependence on dopant type and crystal orientation, two different materials were used: 275 μm thick p-type FZ ⟨1 0 0⟩ wafers, which were double side mirror polished with a base resistivity of 2.5 Ω cm, and 275 μm thick n-type FZ ⟨1 1 1⟩ wafers, which were double side mirror polished too, but with a base resistivity of 3.5 Ω cm. Shortly before nitridation, the wafers received an HF dip to remove the surface oxide. As mentioned above the total process consisted of a NH_3 plasma pretreatment to vary nitridation followed by a-SiN_x:H layer deposition. The latter was the same for all pre-treatments. Both steps in the process were performed using a remote PECVD system. The effective lifetime of the minority carriers, which is determined by the bulk lifetime and surface passivating quality, was measured using symmetric test structures with nitridation and a-SiN_x:H coating on both sides. Samples with nitridation and coating on one side were used to determine Q_f and D_{it} using CV-MIS. NH_3 plasma pre-treatments were carried out at temperatures between 300 and 500 °C.

In Fig. 2A and B the effect of the temperature of a NH_3 plasma on Q_f and D_{it} is shown.

A positive correlation between Q_f and D_{it} is found. It can be seen that already at 300 °C a small effect can be seen, which suggests that the onset of nitridation might start at somewhat lower temperature than suggested by Dai [7]. The nitridation effect can be seen by the increase in Q_f. In Fig. 2B, the effect on the effective SRV is shown. A lower effective SRV, thus better passivation, is obtained when the surface is slightly nitridated and so Q_f values up to about 8×10^{12} cm^{-2} are seen, corresponding to pre-treatment temperatures of 400 °C. In this case and according to Dai et al. [7], NH_2 starts to adhere to the surface, but no insertion of N in the Si–Si bonds takes place. The reduction in effective SRV compared to samples without plasma pre-treatment (nitridation) at 300 °C might be related to the onset of nitridation of the thin native oxide present on the wafer surface. Above 450 °C N insertion into Si–Si takes place, which corresponds to a higher effective SRV and is related to a further increase in Q_f and the now dominant high D_{it}. An optimum was found at 400 °C for n-type ⟨1 1 1⟩ and at 300 °C for p-type ⟨1 0 0⟩. The results clearly show that tuning of the effective SRV is possible, independently of the bulk properties of the SiN_x:H layer.

3. Solar cell study

3.1. Solar cell (semi) fabric processing

Solar cell and semi-fabrics were fabricated on both n-type (mono crystalline Si) and p-type (both multi-Si and mono-Si) to study the effect of the nitridation and fixed charge on the cell output. Semi fabricated Si wafers were textured with an alkaline or acidic procedure for respectively mono- and multi-Si wafers. The emitter (boron for n-type base material and phosphorus for p-type) was fabricated by a high temperature diffusion step. Subsequently, the glass was removed and the wafers were cleaned and passivated with SiN_x:H.

The structures of the fabricated n-type and p-type cells are shown in Fig. 3. For p-type cells the processing started with an alkaline or acidic texture formation for respectively mono- and multicrystalline Si wafers. The emitter was formed using $POCl_3$ diffusion and after glass removal and cleaning the wafers were passivated with SiN_x:H. Screen printing was used to apply the metallization. At the rear side the area was fully printed with aluminum and at the front side a silver H-pattern was used. Contacting is obtained by a co-firing procedure. The n-type cells were made using an alkaline texture, after which the boron emitter and phosphorus back-surface-field are created in a high temperature diffusion step. After glass removal and cleaning, the wafers were passivated on both sides with SiN_x:H. The contacting of the metal pastes was done in a co-firing procedure. The processing is further described in [17] and [18] respectively. Prior to the a-SiN_x:H layer deposition on the front side, the cells are given a plasma NH_3 pre-treatment to alter Q_f and D_{it}.

The square p-type multi-Si wafers were 210 μm thick with a base resistivity of 1.3 Ω cm. The 180 μm thick and square p-type Cz mono-Si had a base resistivity of 1.3 Ω cm. The semi-square n-type Cz mono-Si had a base resistivity of 25 Ω cm and were 180 μm thick. All wafers were sized 156×156 mm^2.

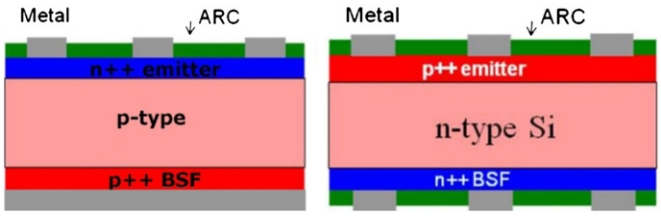

Fig. 3. Structure of a left: standard p-type cell, and a right: bifacial n-type cell.

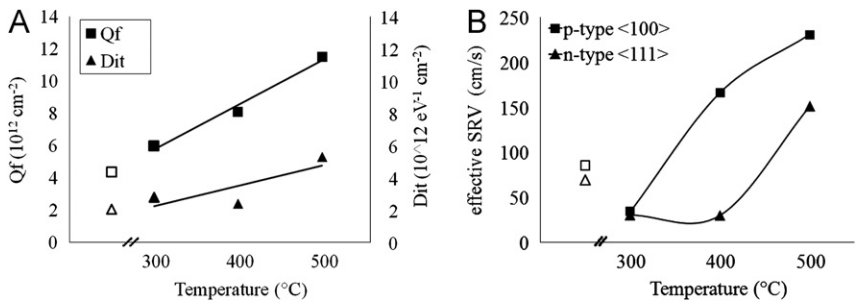

Fig. 2. (A) and (B) The effect of the temperature of a NH_3 plasma treatment on Q_f, D_{it} and effective SRV for a minority carrier density of 1.10^{15} cm^{-3} as measured on p-type ⟨1 0 0⟩. Open and closed symbols are samples without respectively with pre-treatment. The lines are guides to the eye.

3.2. Effect of doping density

Two types of base doping are currently used within the silicon solar cells industry. These are phosphorus (n-type) and boron (p-type). The required emitters of these solar cells are of opposite character to the base doping, respectively boron and phosphorus. For n-type emitters the positive fixed charge of the SiN_x:H will result in accumulation. For p-type emitters the positive fixed charge will result in depletion, and in case of low doping, in inversion, which in final solar cells will induce inversion layer shunting, as shown by Dauwe [19]. The extent of the effect of the surface passivation, significantly depend on the quality of the emitter. High recombination rates in the emitter will reduce any effect of surface passivation to insignificant. This is also reflected in the Shockley–Read–Hall formalism in which the surface recombination significantly depends on the doping density [20]. Therefore, the effect of doping has to be included in order to examine the effect of Q_f on the cell output.

3.3. Relationship Q_f and Implied V_{oc}

The V_{oc} is directly related to passivation and hence this factor has been chosen to show. In Fig. 4, V_{oc} is given as a function of Q_f for n-type cells. As Q_f and D_{it} increase simultaneously with increased nitridation, the trend in V_{oc} is due to the combined effect of increased D_{it} and increased depletion caused by higher Q_f. With increasing positive fixed charge more depletion occurs at the interface, reducing the V_{oc}. Also the effect in other cell parameters like the J_{sc} and *FF* were very significant, with a 20 mV change in V_{oc} a similar trend was shown in J_{sc} and *FF* by an absolute difference of respectively 2 mA/cm^2 and 1% in *FF*. This strong effect, independent of the a-SiN_x:H deposited, shows the extent of the influence of the surface passivation. PC1D simulations of the solar cell were in accordance with the cell results. PC1D simulations of the cell, showed that for negative fixed charges the V_{oc} is not limited by the surface passivation, but by the recombination in the emitter itself.

A similar but reverse observation can be made for p-type solar cells, as shown in Fig. 4. Implied V_{oc} as determined from p-type mono semi-fabricated which had a standard emitter with a high surface doping of 8×10^{20} atoms/cm^3 as determined with Secondary Ion Mass Spectroscopy (SIMS), showed not to be influenced by Q_f due to different nitridations. To illustrate the effect of the maximal doping of the emitter PC1D modeling [21] was done and shown here as a function of the fixed charge. For the simulations a p-type cell was modeled, using a stack of two Gaussian curves for the phosphorus emitter with a constant depth of 300 nm. The base resistivity for the p-type wafer was 1.3 Ω cm. The lifetime of the minority carriers in p-type wafer material was taken to be 200 μs. It can be seen that due to the high doping level of phosphorus and the high recombination rate in the emitter, the dependence on surface passivation is negligible, even surface passivation schemes with negative fixed charges, like shown by Hoex [22], can be used to coat the surface. However, with reducing doping density in the emitter, the sensitivity for the surface passivation increases and with negative fixed charges the V_{oc} will reduce again due to depletion at the interface. For a low doping density of $3 \cdot 10^{18}$ atoms/cm^3 even inversion will occur, but due the concept of inversion layer shunting this will further reduce the solar cell efficiency. This effect of shunting cannot be simulated with PC1D.

4. Modeling of the SiN_x:H/Si interface

Molecular dynamics (MD) simulations of the effect of increased nitridation were performed using de Brito Mota's [23]

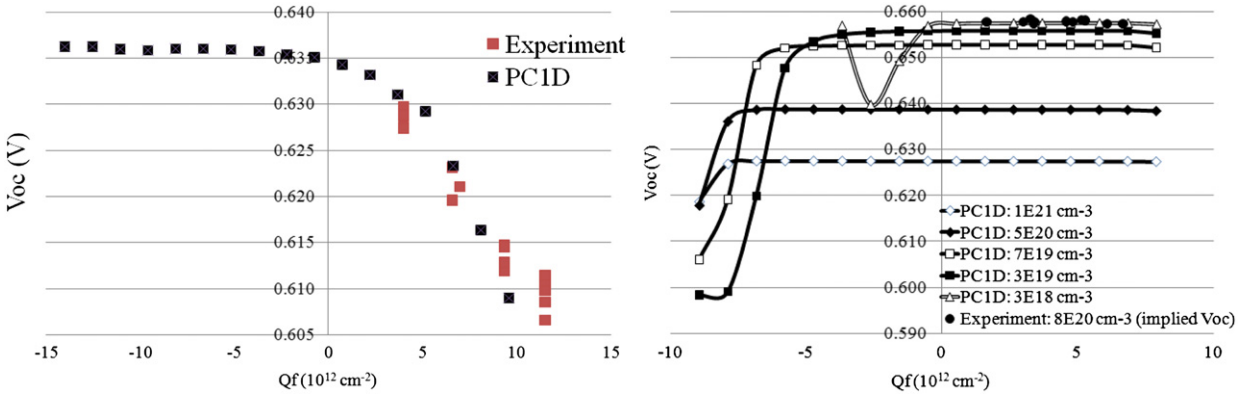

Fig. 4. The V_{oc} of the n-type solar cell (left) and p-type solar cell (right) as function of Q_f, both modeled in PC1D and measured experimentally. For the p-type solar cell the modeling results are given for different values of the phosphorus surface concentration, as well as experimental data for a phosphorus surface concentration of 8×10^{20} atoms/cm^3.

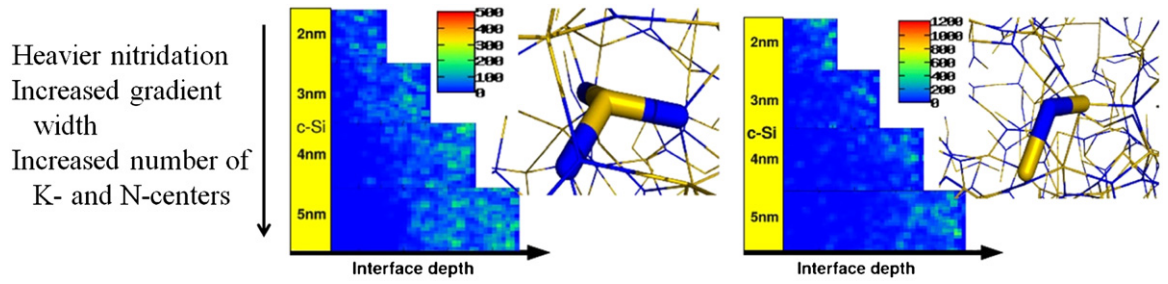

Fig. 5. Molecular Dynamics Simulations of nitridation on: Left: K-centers; Right: N-centers. In the figures the a-SiN_x:H is represented in blue, the c-Si bulk is yellow and the legends refer to the density of K- and N- centers identified by analyzing the simulation trajectories. The subfigures (horizontal and bar-like) in each plot with 2, 3, 4 and 5 nm gradient width show heavier nitridation results in an increased number of K and N centers.

parameterization of the Tersoff potential [24]. Heavier nitridation increases the recombination inside the Si crystal. This correlates with the increased presence of K- and N-centers at the interface as shown in Fig. 5. Since charge carriers will hardly penetrate into the a-SiN_x:H region only the defect centers at the surface will be expected to affect the recombination rates. As the N gradient width is increased from 2 up to 5 nm the defect concentration moves steadily away from the interface. The plots show a clear increase in volume fraction of both the K- and N-centers, which correlate to the experimentally found increase in Q_f and D_{it} due to heavier nitridation. The modeling and results are described in more detail in [25].

5. Conclusions

The incorporation of N into the Si surface is a process called nitridation. This nitridation is closely related to the density of interface states (D_{it}) and fixed charges (Q_f), which are parameters that determine the surface passivation quality in a solar cell. Increasing the nitridation by use of a plasma treatment prior to a-SiN_x:H deposition alters Q_f from 2×10^{12} to 15×10^{12} cm^{-2} and the correlated D_{it} from 2×10^{12} to 16×10^{12} eV/cm^2.

In completed solar cells the effect of the controlled Q_f and D_{it} is studied. On n-type solar cells, due to increased depletion, increases in Q_f and D_{it} resulted in a drop in open-circuit voltage, V_{oc}, of over 20 mV. On p-type solar cells, where the Q_f results in accumulation, the effect was negligible. The effects on both types of solar cells were confirmed with PC1D modeling.

Molecular dynamics modeling of the nitridation effect shows that with increased nitridation the volume and fraction of the K- and N-centers in the Si bulk increase and are located in the first few nm from the interface. This correlates to the experimentally found increase in both Q_f and D_{it}.

Acknowledgements

The authors acknowledge support from the European Commission grant MMP3-SL-2009–228513, "Hipersol" as part of the 7th Framework Package, grant number 228513. Via our membership of the UK's HPC Materials Chemistry Consortium, which is funded by EPSRC (EP/F067496), this work made use of the facilities of HECToR, the UK's national high-performance computing service, which is provided by UoE HPCx Ltd at the University of Edinburgh, Cray Inc and NAG Ltd, and funded by the Office of Science and Technology through EPSRC's High End Computing Programme.

References

[1] I.G. Romijn et al., Proceedings of the 20th European Photovoltaic Solar Energy Conference and Exhibition, Barcelona, 2005, pp. 1352.
[2] H.F.W. Dekkers et al., Proceedings of the 20th European Photovoltaic Solar Energy Conference and Exhibition, Barcelona, 2005, pp. 721.
[3] A.G. Aberle, Crystalline Silicon Solar Cells—Advanced Surface Passivation and Analysis, Publisher: Centre for Photovoltaic Engineering, University of New South Wales.
[4] D.E. Aspnes, American Journal of Physics 50 (1982) 704.
[5] W.L. Warren, et al., Journal of Applied Physics 70 (1991) 2220.
[6] F. Giorgis, et al., Philosophical Magazine B 70 (1998) 925.
[7] M. Dai, et al., Nature Materials 8 (2009) 825.
[8] T. Takakura, et al., Japanese Journal of Applied Physics 49 (2010) 046502.
[9] W. Soppe, et al., Progress in Photovoltaics 13 (2005) 551.
[10] M.W.P.E. Lamers et al., Materials Research Society Fall Meeting, Boston, (2011) d.
[11] F. Demichelos, et al., Philosophical Magazine B 74 (1996) 155–168.
[12] S. Wolf, Journal of Applied Physics 97 (2005) 063303.
[13] V. Verlaan, Silicon Nitride at High Growth Rate Using Hot Wire Chemical Vapor Deposition, Ponsen & Looijen b.v., Wageningen, 2008.
[14] P. Grunow et al., Proceedings of the 46th IEEE Photovoltaic Specialists Conference, 2006, pp. 2152.
[15] M.H. Kang, et al., Progress in Photovoltaics 19 (2011) 983.
[16] H.F.W. Dekkers Study and Optimization of Dry Process Process Technologies For Thin Crystalline Silicon Solar Cell Manufacturing (2008).
[17] M.W.P.E. Lamers, Proceedings of the 23rd European Photovoltaic Solar Energy Conference and Exhibition, 2008, 2CV.5.39.
[18] A.W. Weeber et al., International Workshop on Science and Technology of Crystalline Silicon Solar Cells (CSSC-4), (2010).
[19] S. Dauwe, Low Temperature Surface Passivation of Crystalline Silicon and its Application to the Rear Side of Solar Cells, University of Hannover, 2004.
[20] W. Shockley, et al., Physical Review 87 (1952) 835.
[21] P.A. Basore et al., Proceedings of the 25th IEEE Photovoltiac Specialists Conference, 1996, pp. 377–381.
[22] B. Hoex, et al., Physica Status Solidi. RRL6 (2012) 4–6.
[23] F. de Brito Mota, et al., Journal of Applied Physics 86 (1999) 1843.
[24] J. Tersoff, Physical Review Letters 56 (1986) 632.
[25] K.T. Butler, et al., Journal of Applied Physics 110 (2011) 124905.